PASJ: Publ. Astron. Soc. Japan **59**, 245–261, 2007 February 25

High-Resolution and High-S/N Spectrum Atlas of Vega*

Yoichi TAKEDA, Satoshi KAWANOMOTO, and Naoko OHISHI
National Astronomical Observatory, 2-21-1 Osawa, Mitaka, Tokyo 181-8588
takedayi@cc.nao.ac.jp, kawanomoto.satoshi@nao.ac.jp, naoko.ohishi@nao.ac.jp

(Received 2006 July 31; accepted 2006 December 3)

Abstract

We present a digital spectral atlas of Vega covering from violet to the near-IR region ($\sim$ 3900–8800 Å), which has such a high resolution ($R \sim 100000$) and high signal-to-noise ratio (typically $\sim$ 1000–2000 on the average) as to allow a detailed line-profile analysis. In addition, theoretically simulated spectra and lists of lines predicted to have appreciable strengths are also provided, which may be useful for identifying or searching lines on the atlas. Besides, the spectra of Regulus (a representative rapid rotator) obtained at the same night are appended as a reference of telluric lines.

Key words: atlases — line: profiles — stars: early-type — stars: individual (α Lyr, α Leo) — techniques: spectroscopic

1. Motivation

Vega (= α Lyr = HR 7001 = HD 172167 = HIP 91262, A0 V), one of the most familiar and extensively studied stars, has begun to draw renewed attention of stellar astronomers, thanks to the remarkable development of recent observational techniques. Namely, the discovery of an unusual "flat-bottomed" shape of weak lines, which was revealed for the first time by the ultra-high S/N ($\gtrsim$ 2500) Reticon spectrum obtained at Dominion Astrophysical Observatory (Gulliver et al. 1991), has presented a new picture that the apparently sharp-lined Vega is actually a rapid rotator seen nearly pole-on, and the peculiar line profile may be interpreted as being due to the rotation-induced latitude-dependent variation of the stellar surface properties (Elste 1992; Gulliver et al. 1994; Hill et al. 2004). In fact, this view has received support, at least qualitatively, from a very recent interferometric observation of Vega's surface brightness distribution (Peterson et al. 2006).

This does not mean, however, that we already have a fully satisfactory understanding of this star. As a matter of fact, from a quantitative point of view, no consensus has yet been accomplished regarding the nature of Vega's rotation, since the best solutions of (v_e, i) suggested from these studies differ appreciably from each other: (245 km s^{-1}, 5°.1; Gulliver et al. 1994), (160 km s^{-1}, 7°.9; Hill et al. 2004), and (274 km s^{-1}, 4°.5; Peterson et al. 2006). It is evident that much more work remains to be done in this field.

Above all, detailed line-shape studies on very high quality spectra should be further pursued. We note that the analyses of Gulliver et al. (1994) and Hill et al. (2004) were based on the profiles of only a few selected lines (Fe I 4528.6, Ti II 4529.5, and Fe II 4522.6), only which do not appear to be sufficient to draw a firm conclusion. Rather, to make a further step, it would be necessary to investigate the profiles of a much larger number of well-behaved lines over a much wider wavelength range, because different lines have different sensitivity to a change of the surface condition (e.g., temperature), which makes an attractive and promising subject of research for stellar spectroscopists.

Unfortunately, Gulliver et al.'s (1991) ultra-high-S/N spectrum obtained at Dominion Astrophysical Observatory, which has been exclusively invoked so far by Gulliver et al. (1994) and Hill et al. (2004), has not been placed in the public domain. On the other hand, none of the open-door spectra of Vega, which were published and made available on-line by a few groups, have a sufficient quality for the purpose of line-profile analyses (cf. section 4).

Considering this situation, we decided to collect such high-quality spectral data of Vega as those of Gulliver et al. (1991) based on our own observations at Okayama Astrophysical Observatory, and to publish them as a digital spectrum atlas. In carrying out this project, we paid particular attention to the following points as the guiding principle:

— The atlas should serve as a practically useful data source in a qualitative as well as quantitative sense, such that it is applicable to detailed profile studies of a variety of spectral lines. Hence, the spectrum should cover a wide wavelength range (from violet to near-IR) to enlarge the opportunities of using as many suitable lines as possible, have a sufficiently high resolution ($R \sim 100000$) so as to assure neglecting the effect of the instrumental profile on stellar line profiles, and have substantially high signal-to-noise ratios (preferably $\gtrsim$ 2000) comparable to that of Gulliver et al.'s (1991) Dominion spectrum.
— In order to increase the usability of the atlas, we also present theoretically simulated spectra as well as lists of lines predicted to have appreciable strengths, so that they may be of help in identifying lines or finding suitable lines on the actual spectra. Since little attention appears to have been paid to this task of line-identification

* The large data sets provided only in the machine-readable form (electronic data files) are available at ⟨http://pasj.asj.or.jp/v59/n1/590122/⟩ as well as at ⟨ftp://dbc.nao.ac.jp/DBC/ADACnew/J/other/PASJ/59.245/⟩. site as well as at the FTP site of Astronomical Data Center of NAOJ upon publication.

in most of the stellar spectrum atlases published so far (mostly providing only bare spectra), in spite of its fundamental importance in the stellar spectroscopic analysis, we hope that these supplementary data would serve such a purpose.

Hence, the aim of this paper is to give an account of the details of these data that we established and made available in the form of electronic tables downloadable via the Internet, as described in the following sections 2 through 5.

2. Observational Data

2.1. Observations

Observations of the target star, Vega,[1] were carried out on 2006 May 1–4 using the HIgh-Dispersion Echelle Spectrograph (HIDES; Izumiura 1999) at the coudé focus of the 188 cm reflector at Okayama Astrophysical Observatory (OAO). Equipped with a 4K×2K CCD detector at the camera focus, the HIDES spectrograph enabled us to obtain an echellogram covering a wavelength range of $\sim$ 1200 Å (in the mode of red cross-disperser). Since only very bright stars were involved in this observation, we intended to accomplish a wavelength resolution as high as possible, even if at the sacrifice of an appreciable light loss. We thus used a rather narrow slit width of 100 μm (0.″38), corresponding to a resolving power of $R \sim 100000$.

Analogous to the project of Takeda et al. (2005), where OAO spectra of 160 F–G–K dwarfs/subgiants were published, we selected four target spectral regions: a blue region of $\sim$ 3900–5100 Å (hereinafter referred to as "b"), a green–yellow region of $\sim$ 5000–6200 Å ("g"), a red region of $\sim$ 6000–7200 Å ("r"), and a near-IR region of $\sim$ 7600–8800 Å ("i"). At each night of observation, one of these four wavelength regions was selected in turn as May 1 (region i), 2 (region b), 3 (region g), and 4 (region r).

Among the four observing nights, the region-i observation on May 1 was often bothered by clouds in spite of a reasonably good seeing (1.″2–1.″5), while the region-b observation on the next night of May 2 suffered a considerably poor seeing condition (2.″4–4″), though the sky was superbly clear over the whole night. The observing conditions on the following two nights of May 3–4 (regions g and r) turned out to be satisfactorily fine in terms of both seeing (0.″8–1.″3) and sky-clarity.

The exposure time of one star frame varied from 30 s to 300 s (adequately chosen by requiring that the ADU count per pixel may not exceed the linearity range), depending on the wavelength region as well as on the sky condition. Since we intended to achieve a very high S/N ratio, special attention was paid to obtaining not only a large number of star frames, but also a sufficient number of flat-field frames. The observation log for Vega is summarized in table 1, where the information of individual spectral frames is also given.

2.2. Data Reduction

A first-order reduction of the echelle data was performed following the standard procedures (bias subtraction, finding echelle orders/apertures to extract, scattered-light subtraction, spectra extraction, wavelength calibration using Th–Ar comparison spectra) with the IRAF[2] software package, yielding calibrated one-dimensional spectra consisting of multi-order spectral segments (34/21/16/10 orders for b/g/r/i regions). Then, all of the spectral frames obtained at the same night were co-added to increase the S/N ratio. Hereinafter, we call such primitive spectra of integrated ADU counts at this reduction stage "raw spectra" for convenience. Following the naming convention adopted by Takeda et al. (2005),[3] these four fits-formatted spectra files were labeled as "h172167b060502.fits", "h172167g060503.fits", "h172167r060504.fits", and "h172167i060501.fits". As an example, we show in figure 1 the intensity distribution of these four raw spectra at each spectral region. Note that a few parts of the spectra (e.g., the spurious dip at $\sim$ 5490 Å or $\sim$ 6070 Å) are damaged due to bad columns in the CCD.

The "raw spectra" were further divided by the local continuum by using the IRAF task "continuum", yielding continuum-normalized spectra. Note, however, that an adequate implementation of this task was considerably difficult in several parts of the spectra (e.g., near the spectrum defects, near the edges of the order or of the detector, near the strong absorption feature such as the Balmer lines, overlapping Paschen lines, or overlapping O_2 telluric lines), where the results of this tentative normalization are totally unreliable, and should not be seriously taken.[4]

Then, for the purpose of bringing the wavelength scale of the spectra to the laboratory system, we determined the necessary Doppler corrections by comparing these normalized spectra with the theoretically computed synthetic spectra (cf. subsection 3.1), which turned out to be +25.3 km s^{-1} (May 2, region b), +25.7 km s^{-1} (May 3, region g), +26.6 km s^{-1} (May 4, region r), and +25.4 km s^{-1} (May 1, region i) with

[1] Actually, three first-magnitude stars, Regulus (α Leo), Vega (α Lyr), and Altair (α Aql), were consecutively observed at each night in this order, with observing time of 2–3 hours allocated for each. The observations and the spectra of Regulus will be briefly mentioned in appendix 1. Meanwhile, a line-profile analysis of Altair based on the data obtained in these observations is currently under way, which will be reported elsewhere. Besides, these three stars were also observed through the iodine cell for the case of region-b, -g, and -r observations, in order to study the instrumental profile by analyzing the absorption spectrum due to I_2 molecules superposed on the background of a rapid-rotator spectrum in the 5000–6000 Å region (cf. subsection 2.3).

[2] IRAF is distributed by the National Optical Astronomy Observatories, which is operated by the Association of Universities for Research in Astronomy, Inc. under cooperative agreement with the National Science Foundation, USA.

[3] A "raw spectra" file for a star has a 19-character name of "h??????[bgri]yymmdd.fits", where ?????? is the HD number (filled with zeros if necessary), [bgri] denotes any one character of 'b', 'g', 'r', and 'i' corresponding to the spectral region, and "yymmdd" denotes the observation date. Quite similarly, a "reduced-spectra" file has a 21-character name in which two characters "dn" ('d' and 'n' means "doppler-corrected"and "normalized", respectively) are inserted after the date string (i.e., right ahead of ".fits").

[4] For example, estimating the correct continuum position near the Balmer lines is completely hopeless, since the theoretical simulation (cf. subsection 3.1) suggests that the wing of strong Balmer lines extends over $\sim$ 200 Å (i.e., up to $\sim \pm$ 100 Å from the line center) for this A0 V star (cf. figure 1), which far exceeds the coverage of one spectrum order ($\lesssim$ 100 Å). In order to remedy this problem, we eventually had to apply an appropriate renormalization (i.e., continuum re-adjustment) with the help of theoretical calculations at the final stage, as mentioned in subsection 2.3.

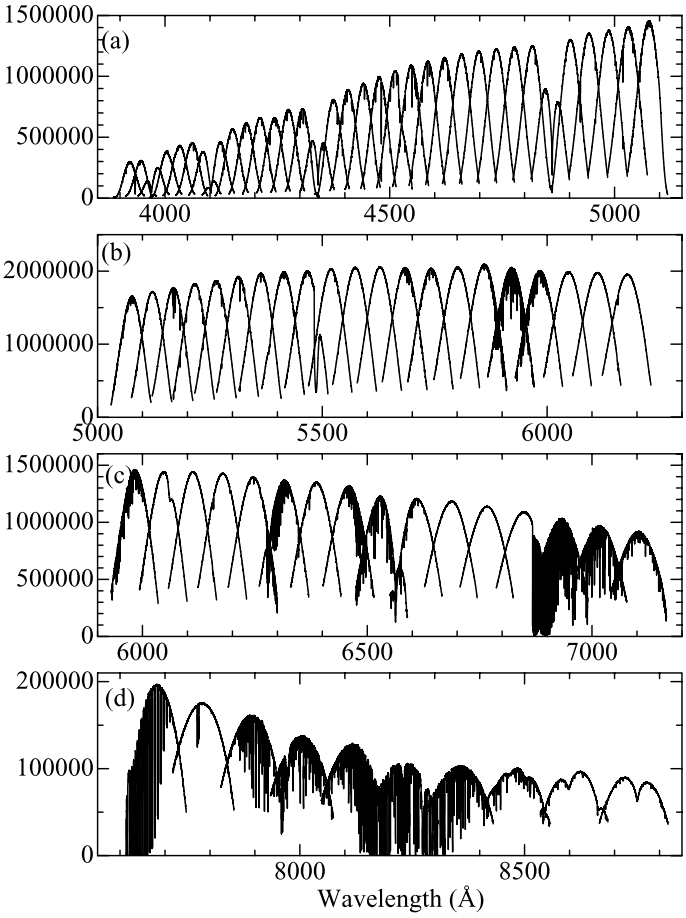

Fig. 1. Panels (a), (b), (c), and (d) show the distributions of accumulated ADU counts for the four "raw spectrum" files of Vega (h172167b060502.fits, h172167g060503.fits, h172167r060504.fits, and h172167i060501.fits; see subsection 2.2 for the definition of the file name), each corresponding to four wavelength regions (b/g/r/i) comprising 34/21/16/10 orders, respectively. The spectrum in each echelle order shows a characteristic intensity distribution corresponding to the blaze function.

a probable precision of $\lesssim 1\,\mathrm{km\ s^{-1}}$. With such determined Doppler shifts, the wavelength scale of each spectra was corrected by using the "dopcor" task of IRAF. Hereinafter, we call such resulting spectra "reduced spectra" for convenience, which were named as "h172167b060502dn.fits", "h172167g060503dn.fits", "h172167b060504dn.fits", and "h172167b060501dn.fits", following Takeda et al.'s (2005) convention.

These eight fits-formatted files (raw and reduced spectra for each of the four wavelength regions) are available in the "fits-files" directory of the electronic data table, where the machine-readable version of table 1 (obslog_vega.txt) is also presented. (See table 5 in section 5 for a summary of the electronic data.)

2.3. *Finally Extracted Spectra and Their Quality*

Based on each fits-formatted file containing reduced spectra, which consists of multi-order spectral segments, we extracted an integrated one spectrum by adequately combining each of the orders (the conjunction wavelengths points were determined by eye-inspection so that the connection may be reasonably smooth).

Although these spectra were tentatively divided by the local continuum level, as mentioned in the previous subsection, their normalization is unreliable in the wings of broad Balmer or Paschen lines, or at $\sim$ 8200–8500 Å where high-n Paschen lines are merged. Therefore, we applied a final continuum-adjustment by further multiplying the spectra by appropriate wavelength-dependent correction-factors (which were determined by carefully comparing the theoretical and tentatively-normalized spectra) so that the appearance of the hydrogen-line features in the resulting observed spectra may become quite similar to the theoretical expectations.[5]

Such arranged final spectra are given in "obspec_?.txt" (? is any of b, g, r, or i). These four text files are available in the "finalspectra" directory of the electronic data table (cf. table 5), and their sample portion is presented in table 2. An overview of these four spectra at each wavelength region is displayed in figure 2, where the theoretically simulated spectra (cf. subsection 3.1) are also shown for a comparison.

Let us check whether our spectra satisfactorily meet the requirement that we originally intended. Since the Gain fac-

[5] Although this procedure implicitly assumes that our theoretical computations of hydrogen-line profiles reliably reproduce the observational data, this was almost confirmed (at least for H α, H β, and H γ) as described in appendix 2. Yet, it should be kept in mind that the continuum levels of our spectra were intentionally adjusted with the help of the theoretical calculations, which means that the resulting hydrogen line features must never be regarded as being genuinely observational.

Table 1. Basic data of Vega observations.

frame#	region	date	UT	sec z	$t_{\rm exp}$ (s)	$\langle count \rangle$
(infrared region: $\langle \sec z \rangle = 1.03$, $\sum \langle count \rangle = 97580$)						
hb63586	i	2006/5/1	17:44:40	1.043	180	14389
hb63587	i	2006/5/1	17:51:44	1.036	300	14240
hb63588	i	2006/5/1	17:59:19	1.029	300	21867
hb63589	i	2006/5/1	18:06:35	1.024	300	11575
hb63590	i	2006/5/1	18:14:00	1.019	300	9444
hb63591	i	2006/5/1	18:21:00	1.014	300	8721
hb63592	i	2006/5/1	18:30:52	1.010	600	17344
(blue region: $\langle \sec z \rangle = 1.33$, $\sum \langle count \rangle = 501153$)						
hb63649	b	2006/5/2	14:51:27	1.533	600	47392
hb63650	b	2006/5/2	15:04:06	1.463	600	57741
hb63651	b	2006/5/2	15:16:02	1.405	600	64320
hb63652	b	2006/5/2	15:27:59	1.353	604	70624
hb63653	b	2006/5/2	15:38:34	1.311	300	32798
hb63654	b	2006/5/2	15:45:45	1.285	300	34074
hb63655	b	2006/5/2	15:52:58	1.261	300	33582
hb63656	b	2006/5/2	15:59:53	1.239	300	35960
hb63657	b	2006/5/2	16:07:05	1.218	300	35082
hb63658	b	2006/5/2	16:21:32	1.179	300	46688
hb63659	b	2006/5/2	16:28:29	1.162	300	42894
(green–yellow region: $\langle \sec z \rangle = 1.28$, $\sum \langle count \rangle = 1322662$)						
hb63750	g	2006/5/3	14:37:50	1.593	60	47371
hb63751	g	2006/5/3	14:41:47	1.568	30	20788
hb63752	g	2006/5/3	14:44:45	1.550	30	21418
hb63753	g	2006/5/3	14:47:06	1.536	30	24070
hb63754	g	2006/5/3	14:49:26	1.522	30	21868
hb63755	g	2006/5/3	14:51:47	1.509	30	21048
hb63756	g	2006/5/3	14:54:07	1.496	30	23413
hb63757	g	2006/5/3	14:56:55	1.481	30	19482
hb63758	g	2006/5/3	14:59:16	1.468	30	21063
hb63759	g	2006/5/3	15:01:37	1.456	30	20170
hb63760	g	2006/5/3	15:03:57	1.444	30	19205
hb63761	g	2006/5/3	15:06:18	1.433	30	19098
hb63762	g	2006/5/3	15:09:02	1.420	30	16964
hb63763	g	2006/5/3	15:11:22	1.409	30	17669
hb63764	g	2006/5/3	15:13:43	1.398	30	18092
hb63765	g	2006/5/3	15:16:04	1.387	30	21931
hb63766	g	2006/5/3	15:18:24	1.377	30	22740
hb63767	g	2006/5/3	15:21:10	1.365	30	21251
hb63768	g	2006/5/3	15:23:30	1.355	30	18167
hb63769	g	2006/5/3	15:25:51	1.346	30	19988
hb63770	g	2006/5/3	15:28:12	1.336	30	18719
hb63771	g	2006/5/3	15:30:32	1.327	30	22511
hb63772	g	2006/5/3	15:33:31	1.316	30	21014
hb63773	g	2006/5/3	15:35:51	1.307	30	18305
hb63774	g	2006/5/3	15:38:12	1.298	30	18651
hb63775	g	2006/5/3	15:40:33	1.290	30	20738
hb63776	g	2006/5/3	15:42:53	1.282	30	22626
hb63777	g	2006/5/3	15:45:45	1.272	30	21312
hb63778	g	2006/5/3	15:48:06	1.264	30	19983
hb63779	g	2006/5/3	15:50:27	1.257	30	23220
hb63780	g	2006/5/3	15:52:47	1.249	30	22753
hb63781	g	2006/5/3	15:55:08	1.242	30	22048
hb63782	g	2006/5/3	15:58:35	1.231	30	22638
hb63783	g	2006/5/3	16:00:55	1.224	30	18172
hb63784	g	2006/5/3	16:03:16	1.218	30	19297
hb63785	g	2006/5/3	16:05:37	1.211	30	18822
hb63786	g	2006/5/3	16:07:57	1.204	30	18603
hb63787	g	2006/5/3	16:12:19	1.193	60	34073

Table 1. (Continued.)

frame#	region	date	UT	$\sec z$	$t_{\rm exp}$ (s)	$\langle count \rangle$
hb63788	g	2006/5/3	16:15:10	1.185	60	37452
hb63789	g	2006/5/3	16:18:01	1.178	60	34687
hb63790	g	2006/5/3	16:20:51	1.171	60	42130
hb63791	g	2006/5/3	16:23:42	1.164	60	36761
hb63792	g	2006/5/3	16:26:58	1.157	60	35322
hb63793	g	2006/5/3	16:29:49	1.150	60	37937
hb63794	g	2006/5/3	16:32:39	1.144	60	45159
hb63795	g	2006/5/3	16:35:30	1.138	60	53177
hb63796	g	2006/5/3	16:38:21	1.132	60	45714
hb63797	g	2006/5/3	16:41:43	1.125	40	26250
hb63798	g	2006/5/3	16:44:13	1.120	40	23718
hb63799	g	2006/5/3	16:46:44	1.116	40	24629
hb63800	g	2006/5/3	16:49:15	1.111	40	25284
hb63801	g	2006/5/3	16:51:45	1.106	40	35159
(red region: $\langle \sec z \rangle = 1.29$, $\sum \langle count \rangle = 898831$)						
hb63980	r	2006/5/4	14:42:10	1.542	60	7433
hb63981	r	2006/5/4	14:46:45	1.515	180	21495
hb63982	r	2006/5/4	14:51:48	1.487	180	68834
hb63983	r	2006/5/4	14:55:58	1.465	60	18657
hb63984	r	2006/5/4	15:01:28	1.437	90	42595
hb63985	r	2006/5/4	15:05:48	1.416	90	46854
hb63986	r	2006/5/4	15:11:30	1.390	60	38545
hb63987	r	2006/5/4	15:14:21	1.378	60	34783
hb63988	r	2006/5/4	15:17:11	1.365	60	34849
hb63989	r	2006/5/4	15:20:02	1.353	60	29322
hb63990	r	2006/5/4	15:22:53	1.342	60	25314
hb63991	r	2006/5/4	15:26:33	1.327	60	28991
hb63992	r	2006/5/4	15:29:23	1.316	60	18847
hb63993	r	2006/5/4	15:32:14	1.306	60	10809
hb63994	r	2006/5/4	15:35:05	1.296	60	10630
hb63995	r	2006/5/4	15:37:55	1.285	60	22825
hb63996	r	2006/5/4	15:41:13	1.274	60	17030
hb63997	r	2006/5/4	15:44:04	1.265	60	15177
hb63998	r	2006/5/4	15:46:54	1.255	60	9537
hb63999	r	2006/5/4	15:49:45	1.246	60	5693
hb64000	r	2006/5/4	15:52:35	1.238	60	17777
hb64001	r	2006/5/4	15:57:01	1.224	60	5384
hb64002	r	2006/5/4	15:59:52	1.216	60	10821
hb64003	r	2006/5/4	16:02:42	1.208	60	9439
hb64004	r	2006/5/4	16:05:33	1.200	60	24582
hb64005	r	2006/5/4	16:08:23	1.193	60	29443
hb64006	r	2006/5/4	16:11:49	1.184	60	21311
hb64007	r	2006/5/4	16:14:39	1.177	60	10178
hb64008	r	2006/5/4	16:17:30	1.170	60	5849
hb64009	r	2006/5/4	16:20:20	1.163	60	11091
hb64010	r	2006/5/4	16:23:11	1.156	60	17496
hb64011	r	2006/5/4	16:28:18	1.145	120	45096
hb64012	r	2006/5/4	16:32:09	1.137	120	35817
hb64013	r	2006/5/4	16:35:59	1.129	120	35054
hb64014	r	2006/5/4	16:39:50	1.121	120	56711
hb64015	r	2006/5/4	16:43:41	1.114	120	54563

Presented here are the observation logs of each individual spectrum frame of Vega: The frame number, wavelength region index, observation date, UT (at the mid-exposure), air mass, exposure time (in second), and the mean ADU count (obtained by applying the IRAF task "imstatistics" to the extracted 1D echelle spectrum image). The mean value of $\sec z$ (weighted according to each $\langle count \rangle$) and the sum of $\langle count \rangle$, corresponding to the final spectrum derived by co-adding all the spectra at the same night/region, are also given.

Table 2. Sample portion of the final Vega spectrum.

λ (1)	residual (2)	count (3)	S/N (4)	aperture (5)	order (6)	(location) (7)
3900.0028	0.67582	72845	553	34	145	(22%)
3900.0200	0.67744	73159	554	34	145	(22%)
3900.0372	0.67705	73258	555	34	145	(22%)
3900.0544	0.68024	73743	557	34	145	(22%)
3900.0716	0.68273	74156	558	34	145	(22%)
3900.0888	0.68133	74143	558	34	145	(22%)
3900.1060	0.68173	74326	559	34	145	(22%)
3900.1232	0.68420	74739	560	34	145	(22%)
3900.1404	0.68362	74816	561	34	145	(22%)
3900.1576	0.68186	74767	560	34	145	(22%)
3900.1748	0.68303	75035	561	34	145	(22%)
3900.1920	0.68032	74880	561	34	145	(22%)
3900.2092	0.67575	74515	559	34	145	(22%)
3900.2264	0.66986	74003	558	34	145	(22%)
3900.2436	0.66448	73549	556	34	145	(22%)
3900.2608	0.65662	72814	553	34	145	(22%)
3900.2780	0.64607	71779	549	34	145	(22%)
3900.2952	0.63857	71078	546	34	145	(22%)
3900.3124	0.62608	69818	542	34	145	(22%)
3900.3296	0.61164	68334	536	34	145	(22%)

In order to describe the data format of the four files ("obspec_b.txt", "obspec_g.txt", "obspec_r.txt", and "obspec_i.txt") containing the final Vega spectrum at each wavelength region (see the text in subsection 2.3 for more details), the first 20 lines of "obspec_b.txt" are shown here as an example. The spectra are presented in an (order-dependent) wavelength step of 0.017–0.022 Å (region b), 0.022–0.027 Å (region g), 0.026–0.031 Å (region r), and 0.034–0.038 Å (region i); one line corresponding to one wavelength point. The meanings of each of the seven columns are as follows: (1) the wavelength in Å (the radial velocity correction had already been applied so that the wavelengths of stellar lines coincide with the laboratory values), (2) residual intensity (spectrum count divided by the local continuum), (3) spectrum count (in ADU), (4) signal-to-noise ratio estimated by the formula of S/N $\equiv (4.2 \times count)^{1/2}$, (5) aperture number of the original fits-file (e.g., h172167b060502dn.fits for the case of region b) from which this spectrum portion was extracted, (6) echelle order corresponding to this aperture, and (7) position of the spectrum point within the relevant echelle order (0% at the short-wavelength edge, $\sim 50\%$ around the middle point, and 100% at the long-wavelength edge).

tor of CCD is 4.2 e^-/ADU, the local signal-to-noise ratio can be theoretically estimated as $\mathrm{S/N} \equiv (4.2 \times count)^{1/2}$, where *count* is the integrated intensity of the "raw" spectra at each wavelength. Plots of such evaluated S/N values against the wavelength are shown in figure 3, where we can see that S/N $\sim$ 1000–3000 is accomplished for the region-b/g/r spectra (while S/N at region i remains at only $\sim$ 500–1000). We also confirmed from a direct measurement ('m' command of the "splot" task in IRAF) that S/N $\gtrsim$ 2000 is actually realized at the best efficiency region.

In order to evaluate the attained value of the resolving power, we determined the FWHM of the instrumental profile (assumed to be Gaussian) by applying the technique described in Takeda et al. (2002; cf. subsection 3.5 therein) to each 5 Å-chunk of the I_2-contaminated spectrum of Regulus (rapid rotator; cf. footnote 1) at 5000–6000 Å (which is mainly relevant to the spectrum at region g, and partly at regions b and r). The results are depicted in figure 4. It can be recognized from this figure that an FWHM of $\sim 3\,\mathrm{km\ s^{-1}}$, corresponding to the resolution of $R \equiv c/\mathrm{FWHM} \simeq 3 \times 10^5/3 \simeq 100000$, is actually accomplished.

3. Theoretical Simulation

3.1. Spectrum Synthesis

The calculation of theoretical synthetic spectra, which are intended to be compared with the observed spectra of Vega, was carried out as follows. Regarding Vega's atmospheric parameters (the effective temperature, surface gravity, microturbulence, metallicity), we adopted $T_{\mathrm{eff}} = 9550$ K, $\log g = 3.95$, $v_{\mathrm{t}} = 2\,\mathrm{km\ s^{-1}}$, and [M/H] = -0.5, according to Castelli and Kurucz (1994); and the model atmosphere corresponding to these parameters was constructed by interpolating the grid of ATLAS9 models (Kurucz 1993).[6] Including all of the atomic line data given in the extensive compilation of Kurucz and Bell (1995),[6] we synthesized the theoretical absolute (H_λ^0) and normalized ($H_\lambda^0/H_{\mathrm{c}}$) the stellar flux spectra for the relevant four wavelength regions, where H_{c} is the continuum flux and the superscript "0" denotes that no macro-broadening is included. As for the spectrum synthesis program, we used SPTOOL, which was developed by Y. Takeda based on Kurucz's (1993)[6] ATLAS/WIDTH code. LTE was assumed throughout these calculations. Regarding the computations of hydrogen lines, our calculation used realistic Stark profiles based on the VCS theory (Vidal et al. 1973) as far

[6] ⟨http://kurucz.harvard.edu/cdroms.html⟩

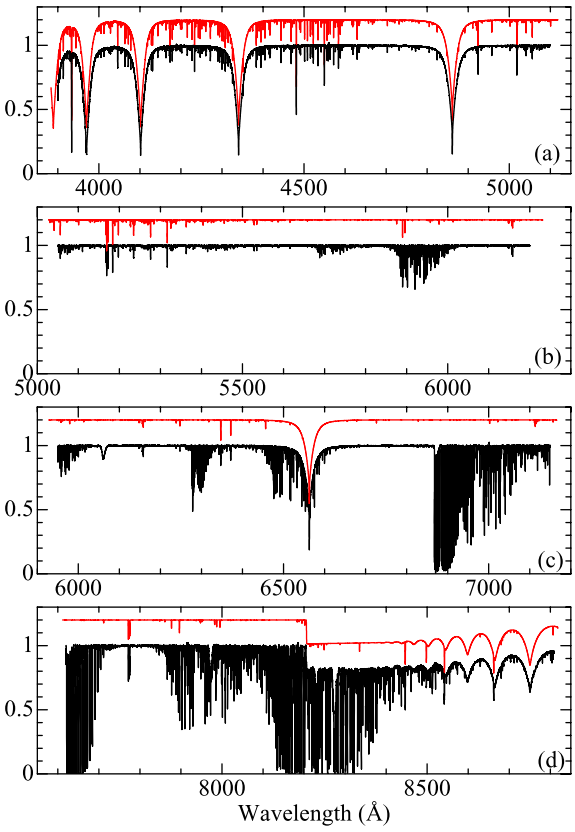

Fig. 2. Analogous to figure 1, panels (a), (b), (c), and (d) show the spectral intensity distributions of the four "finally arranged spectrum" files of Vega (obspec_b.txt, obspec_g.txt, obspec_r.txt, and obspec_i.txt; see subsection 2.3 and table 2 for more details). In addition, theoretically synthesized spectra that have been computed and rotationally broadened with $v_e \sin i = 20$ km s^{-1} (i.e., H_λ^{20}/H_c contained in the four "theocomb_?.txt" files; cf. subsection 3.1 and table 3) are also shown by red lines for a comparison (colored only in the electronic edition) with an upward offset of +0.2 to avoid confusion. Note that the continuum-normalization of these observed spectra was eventually done with the help of theoretical calculations (also shown here), owing to the difficulties of correctly placing the continuum in the broad wings of strong Balmer lines or in the region of overlapping Paschen lines. [cf. subsection 2.3].

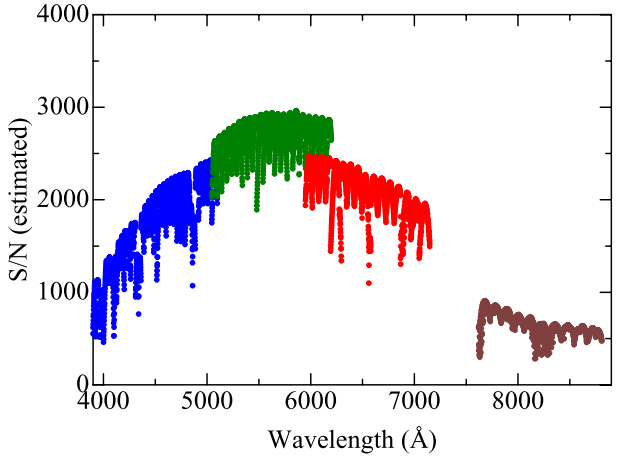

Fig. 3. Plot of the signal-to-noise ratio estimated from ADU counts of the raw spectra shown in figure 1 (the data "S/N" contained in the four "obspec_?.txt" files; cf. the caption in table 2) against the wavelength. The results for region b/g/r/i are shown in blue/green/red/brown, respectively [colored only in the electronic edition].

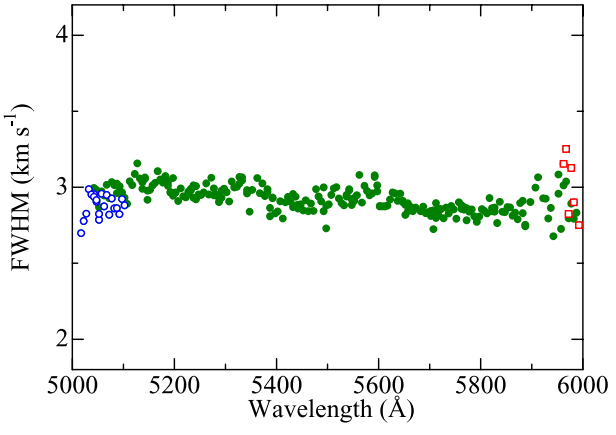

Fig. 4. Plot of the FWHM values (in km s^{-1}) of the instrumental profile against the wavelength, which were evaluated from the Gaussian-fit analysis of (many 5 Å chunks of) the I_2-contaminated spectrum of α Leo (rapid rotator) between 5000 Å and 6000 Å. The results from the spectra of region b, region g, and region r are shown by blue open circles, green filled circles, and red open squares, respectively. [colored only in the electronic edition].

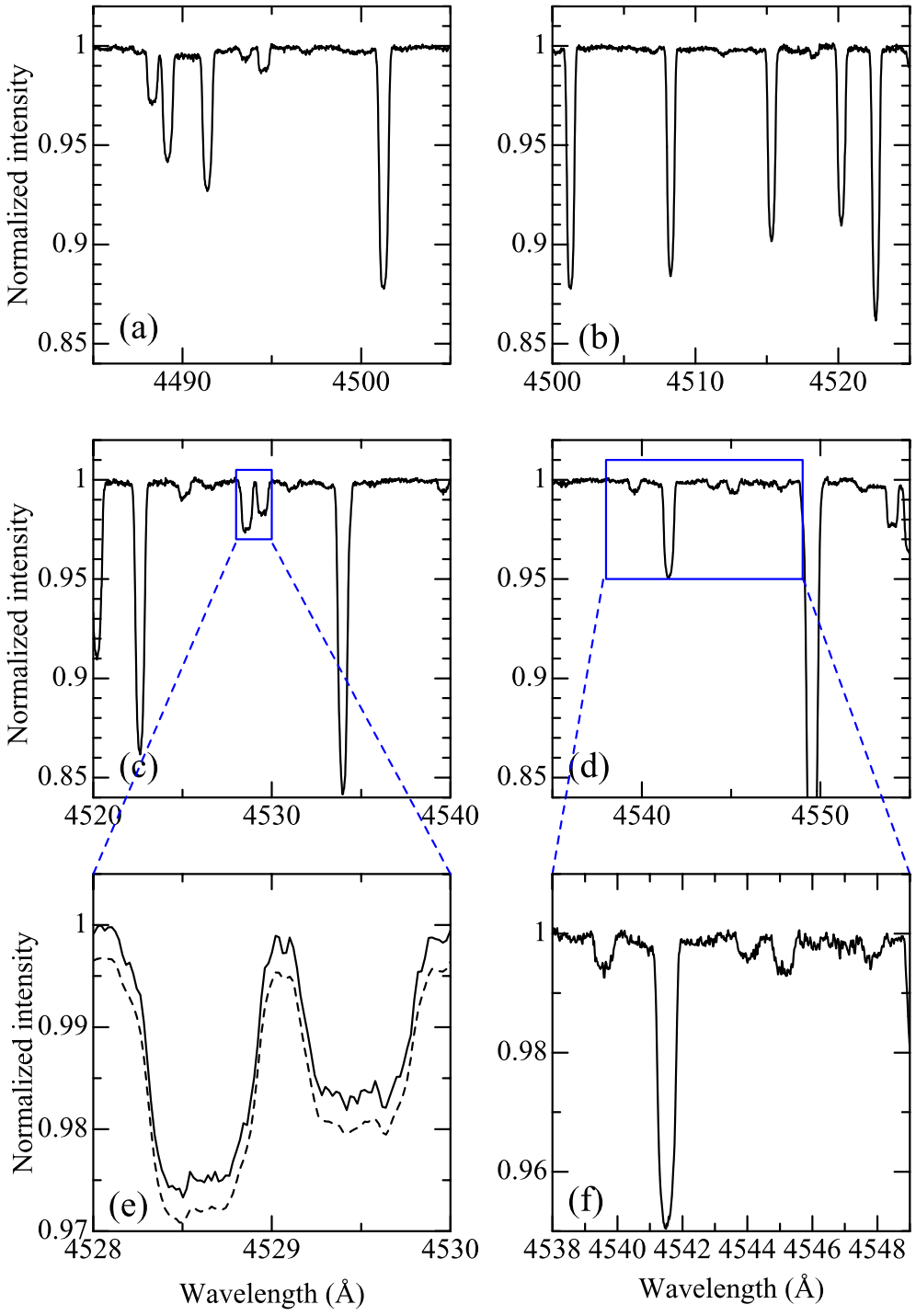

Fig. 5. Six selected portions of our region-b spectrum (obspec_b.txt) around $\sim$ 4500 Å: (a) 4485–4505 Å, (b) 4500–4525 Å, (c) 4520–4540 Å, (d) 4535–4555 Å, (e) 4428–4530 Å, and (f) 4538–4549 Å. In order to enable direct comparisons with Gulliver et al.'s (1991) ultra-high Vega spectra obtained at Dominion Astrophysical Observatory, the ranges of the abscissa/ordinate of these panels (a)–(f) are chosen as to coincide with those of their figures 1a, 1b, 1c, 1d, 3, and, 2, respectively. Regarding panel (e), an additional spectrum smoothed by applying a 3-pixel boxcar function is also shown by a dashed line (with a downward offset of −0.003).

as available; i.e., application of the data in the BALMER program (Kurucz 1993)[6] four the first four Balmer lines (H α, H β, H γ, and H δ) and the data published by Lemke (1997) for the Paschen lines. Otherwise, the original treatment adopted in the ATLAS model-atmosphere program (cf. Kurucz 1970), which was based on Griem's (1960, 1967) theory, was applied. These spectra were further convolved with the rotational broadening function corresponding to $v_{\rm e} \sin i = 20\,{\rm km\ s^{-1}}$ to obtain H_λ^{20} and $H_\lambda^{20}/H_{\rm c}$,[7] where the limb-darkening coefficient was as-

[7] We adopted 20 km s^{-1} as the projected rotational velocity ($v_{\rm e} \sin i$) of Vega, which is the mean of 15 km s^{-1} (Abt & Morrell 1995) and 25 km s^{-1} (Royer et al. 2002).

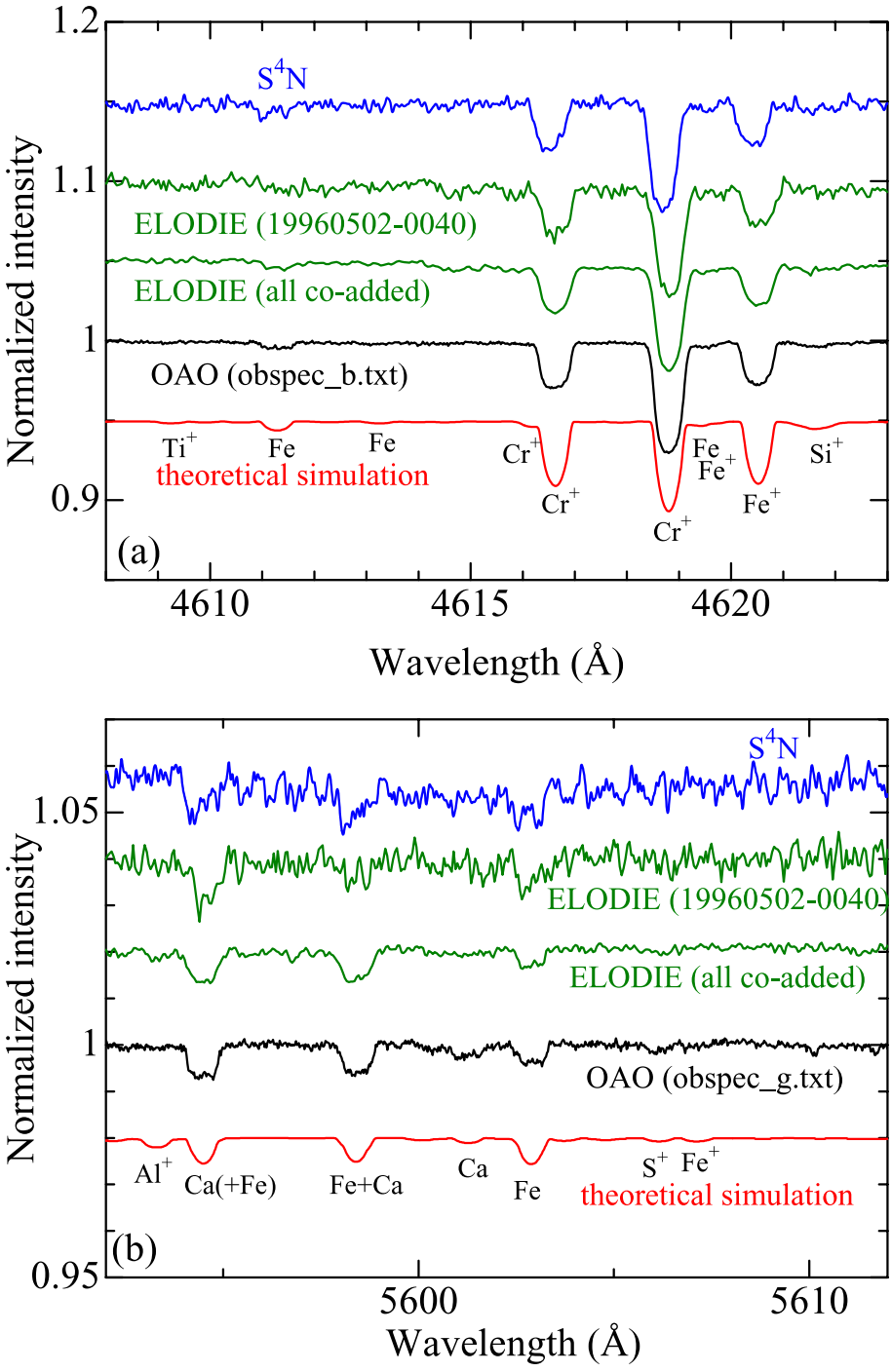

Fig. 6. Comparison of our Vega spectrum (black line) with those of other groups, which are placed in the public domain: Allende Prieto et al.'s (2004) data published as a result of their S^{4}N project (blue lines), the spectra of ELODIE archive (Moultaka et al. 2004) where two kinds of spectra (the highest-class S/N spectrum among the available ones and the all-combined spectrum co-added by ourselves) are shown here (green lines). In addition, as in figure 2, theoretically synthesized spectra that have been computed and rotationally broadened with $v_e \sin i = 20\,\mathrm{km\ s^{-1}}$ are also depicted for a comparison (red lines). Each spectrum is vertically offset by an appropriate amount (0.05, 0.02, 0.05, and 0.2 for panels a, b, c, and d, respectively) relative to the adjacent ones. [Figures are colored only in the electronic edition.]

sumed to be 0.5. Such broadened normalized spectra, H_λ^{20}/H_c, are displayed for reference[8] in figures 2, 5, 6, and 7 along with

[8] Note that these simulated spectra are nothing but an auxiliary tool for rough comparison or line-identification purposes, and that no effort was made to accomplish any quantitative fit. Inconsistencies are often caused by the incompleteness and errors in the adopted gf values. In addition, while the abundances of all elements were assumed to be the reduced solar values by −0.5 dex (represented by [Fe/H]). it is known that some elements do not conform to the deficiency of Fe-group elements in the atmosphere of Vega (e.g., the abundances of C or O, for which the deficiency is more mild and nearer to the solar composition; e.g. Takeda 1993). This fact, coupled with neglecting the non-LTE effect which gen-

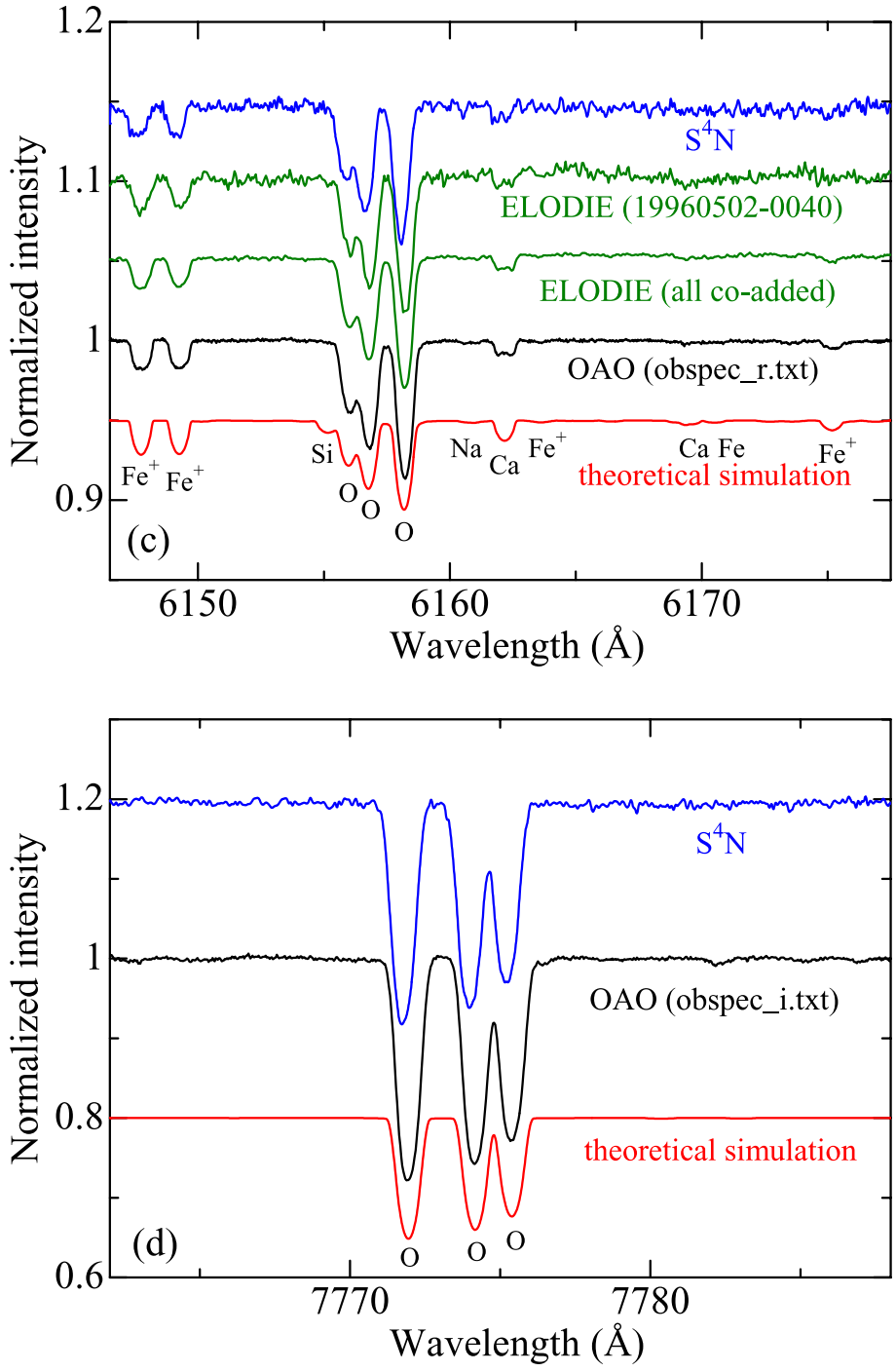

Fig. 6. (Continued.)

the observed spectra of Vega. The resulting four kinds of theoretical spectra (H_λ^0, H_λ^0/H_c, H_λ^{20}, and H_λ^{20}/H_c) at the four wavelength regions are available as the "theocomb_?.txt" files (? is any of b, g, r, and i) in the "synthespec" directory of the electronic data table (cf. table 5). The sample portion of these files is presented in table 3.

erally strengthens near-IR lines of C and O, explains the appreciable discrepancies (i.e., insufficient strengths of simulated lines) seen in figures 6c, d, and 7.

3.2. *Line-Strengths Prediction for Identification*

Now that the theoretical spectra have been calculated, the next task is to provide information for identifying individual spectral lines responsible for the appreciable features on the computed spectra. For this purpose, we use the ratio of the line-center opacity to the continuum opacity, $\eta_0(\equiv l_0/\kappa_c)$ (the subscript "0" means the quantity at the line center), at the reference optical depth of $\tau_{5000} \simeq 0.2$ (assumed to be the representative line-forming depth) as the strength-measure of a line. Since

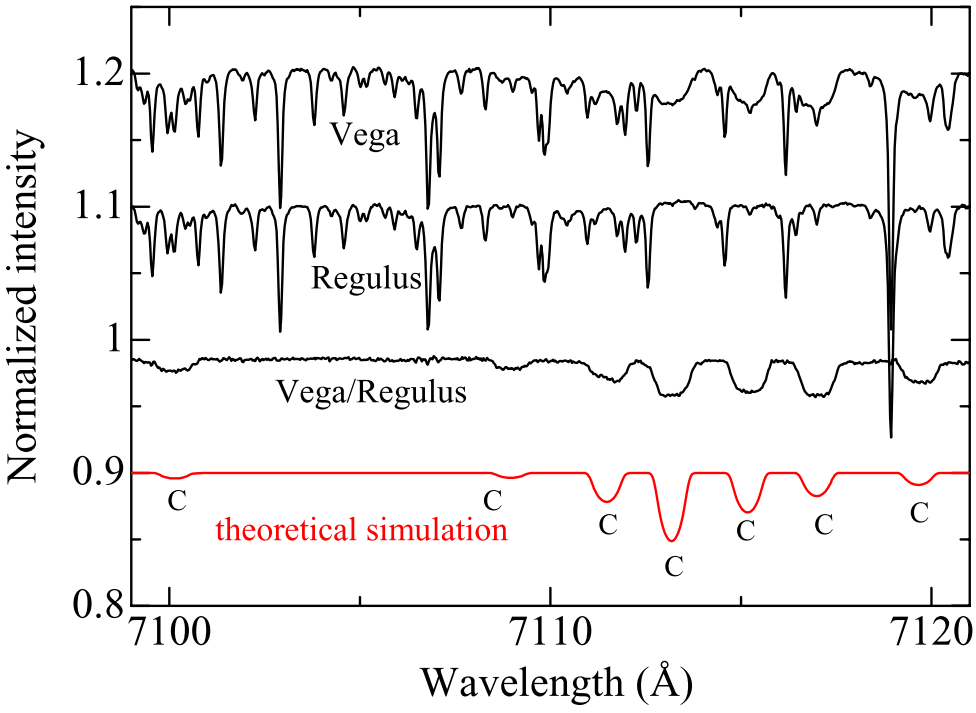

Fig. 7. Demonstration of removing telluric-lines by dividing the target spectrum (Vega) by that of a rapid rotator (Regulus) in the selected 7100–7120 Å wavelength region comprising C I lines, which is contaminated by lines of water vapor in the Earth's atmosphere. Shown here from top to bottom are the spectrum portions for Vega (h172167r060504dn.fits; cf. section 2.2), Regulus (h087901r060504Dn.fits; cf. the appendix 1), the finally divided result of Vega/Regulus (obtained by IRAF task "telluric"), and the theoretical simulation (with a rotationally broadening of $v_{\rm e}\sin i = 20\,{\rm km\,s^{-1}}$). Each spectrum is vertically offset by 0.1 relative to the adjacent ones.

we know that the depth of a line profile, $R_\lambda(\equiv 1 - F_\lambda/F_{\rm c})$, is approximately expressed as $R_\lambda \sim \eta_\lambda/(1+\eta_\lambda)$ (Minnaert's formula; see, e.g., Pagel 1997), $R_0(\equiv 1 - F_0/F_{\rm c}) \simeq \eta_0/(1+\eta_0) \sim \eta_0$ holds if $\eta_0 \ll 1$. Accordingly, η_0 can be regarded as being a good indicator for the line-center depth of the computed unbroadened normalized spectrum ($H_0^0/H_{\rm c}$ in subsection 3.1), at least for weak lines.

The computed η_0 values for each of the spectral lines at the four wavelength regions, which resulted as natural by-products of the spectrum-synthesis calculation in subsection 3.1, are available as the "idinfo_?.txt" files (? is any of b, g, r, and i) in the "lineprediction" directory of the electronic data table (cf. table 5). In these files, the detailed line data adopted in the calculations are also presented, which were taken exclusively from the compilation of Kurucz and Bell (1995).[9] Note that we presented only those lines satisfying the condition $\eta_0 \geq 10^{-5}$, without showing lines of negligible contributions. The sample portion of these data files is presented in table 4.

4. Comparisons with the Vega Spectra of Other Groups

In this section we briefly discuss various other Vega spectra published so far, in comparison with those established in this study. We restrict our discussion to only "high-dispersion" spectra (ca. $R \gtrsim 30000$) obtained with efficient "electronic solid-state" detectors (e.g., Reticon, CCD).[10]

4.1. *DAO Ultra-High S/N Spectrum*

We begin with the breakthrough-accomplished Reticon spectrum of Gulliver et al. (1991) in the first place, which was actually the "targeted" data in this study. Their spectrum discussed in that paper, being confined to the portion around $\sim$ 4500 Å, has a wavelength resolution of $R \sim 60000$ and an ultra-high S/N ratio of $\gtrsim 2500$. We show six portions of our region-b spectra in figures 5a, b, c, d, e, and f in the same layout as Gulliver et al.'s (1991) figures 1a, b, c, d, 3, and 2, so that they may be directly compared with each other. We must admit that the S/N ratios of our spectra at this region ($\sim$ 1500–2000; cf. our figure 3) are inferior to theirs ($\gtrsim 2500$); actually, the noise is more appreciable in our case. Yet, since the characteristic flat-bottom feature is surely noticeable, our spectra would be sufficiently usable for detailed studies of line profiles. Further, we would remark that our wavelength step (0.02 Å) is almost twice as small as theirs (0.035 Å), reflecting the difference in the resolving power. Therefore, we can

[9] Regarding the damping parameters, when data are not given in Kurucz and Bell (1995), tentative values were computed following the default treatment of the WIDTH program (cf. Leusin, Topil'skaya 1987).

[10] We would remark that "The Library of Digitized Stellar Spectra Derived from the OAO Spectrophotographic Plates" (Kato et al. 2000) includes the spectrum of Vega as one of their 105 program stars (B0–F7). Though such classical plate-based spectra are far from being usable for detailed line-profile studies in spite of their high-class quality within the framework of traditional photographic observations, these data may be of historical importance and worth visiting to experience the atmosphere of old-day stellar spectroscopy a quarter century ago.
⟨http://www.sci-museum.kita.osaka.jp/~kato/pub10k.html⟩ (paper),
⟨http://www.sci-museum.kita.osaka.jp/~kato/sp_oao1.zip⟩ (data)

Table 3. Sample portion of the synthesized theoretical spectrum.

λ (1)	H_λ^0 (2)	H_λ^0/H_c (3)	H_λ^{20} (4)	H_λ^{20}/H_c (5)
3883.300	5.7173E+06	0.4592	5.8498E+06	0.4698
3883.320	5.8071E+06	0.4664	5.8390E+06	0.4690
3883.340	5.8467E+06	0.4696	5.8283E+06	0.4681
3883.360	5.8462E+06	0.4695	5.8178E+06	0.4673
3883.380	5.8359E+06	0.4687	5.8075E+06	0.4664
3883.400	5.8235E+06	0.4677	5.7974E+06	0.4656
3883.420	5.8106E+06	0.4667	5.7875E+06	0.4648
3883.440	5.7996E+06	0.4658	5.7779E+06	0.4641
3883.460	5.7902E+06	0.4651	5.7685E+06	0.4633
3883.480	5.7801E+06	0.4643	5.7595E+06	0.4626
3883.500	5.7690E+06	0.4634	5.7507E+06	0.4619
3883.520	5.7576E+06	0.4625	5.7422E+06	0.4612
3883.540	5.7463E+06	0.4616	5.7342E+06	0.4606
3883.560	5.7350E+06	0.4607	5.7268E+06	0.4600
3883.580	5.7236E+06	0.4598	5.7193E+06	0.4594
3883.600	5.7121E+06	0.4588	5.7104E+06	0.4587
3883.620	5.7000E+06	0.4579	5.6999E+06	0.4579
3883.640	5.6879E+06	0.4569	5.6887E+06	0.4570
3883.660	5.6768E+06	0.4560	5.6774E+06	0.4561
3883.680	5.6659E+06	0.4551	5.6661E+06	0.4552

In order to describe the data format of the four files ("theocomb_b.txt", "theocomb_g.txt", "theocomb_r.txt", and "theocomb_i.txt") containing the theoretically synthesized Vega spectrum at each wavelength region (see subsection 3.1 for more details), the first 20 lines of "theocomb_b.txt" are shown here as an example. The spectra are presented in a step of 0.02 Å; one line corresponding to one wavelength point. The meanings of each of the five columns are as follows: (1) the wavelength in Å, (2) monochromatic Eddington flux at the stellar surface [$H_\lambda \equiv (1/2)\int_{-1}^{+1} I_\lambda d\mu$] in units of erg cm^{-2} s^{-1} Å^{-1} (without any broadening), (3) theoretical spectrum normalized with respect to the local continuum (without any broadening), (4) monochromatic Eddington flux at the stellar surface convolved with a rotational broadening function of $v_e \sin i = 20$ km s^{-1}, and (5) rotationally-broadened (with $v_e \sin i = 20$ km s^{-1}) theoretical spectrum normalized with respect to the local continuum.

further smooth our spectrum by convolving it with a boxcar function, which may further reduce the superficial noise while keeping the spectral resolution at a level comparable to theirs. An example of such a smoothing process is shown in figure 5e (see the dashed line therein).

4.2. *S^{4}N Project Spectrum*

Somewhat surprisingly, it appears that there are only two public-domain high-dispersion spectra of Vega which are electronically available, so far as we have searched.

One is that of the S^{4}N (Survey of Stars in the Solar Neighborhood) project published by Allende Prieto[11] et al. (2004). Their spectrum, observed at McDonald Observatory, has a resolving power of $R \sim 50000$ and covers a markedly wide wavelength range from $\sim$ 3600 Å to $\sim$ 10400 Å. We note that their spectrograms were fairly well processed (e.g., in terms of combination of different orders, continuum-normalization, etc.) compared with ours. However, the S/N ratio of their spectrum is estimated to be only several hundred ($\sim$ 300–500), which is insufficient for studying the detailed line shape of spectral lines. In this respect, our spectra are more advantageous, as shown in figures 6a, b, c, and d, where our OAO data at four selected spectral segments (each taken from region b, g, r, and i, respectively) are compared with theirs (blue lines).

4.3. *ELODIE Spectrum*

Meanwhile, the other on-line available digital spectrum of Vega is that included in the stellar spectrum library based on observations with the ELODIE spectrograph[12] at the Observatoire de Haute-Provence (Moultaka et al. 2004). Their spectra cover the wavelength range from $\sim$ 3900 Å to $\sim$ 6800 Å, and have a resolution of $R \sim 42000$. A total of 40 public spectra of Vega were obtained from their archive, though we had to apply some extra data-processing to these, as described below.

Having checked each of these, we discarded three spectra (20000808/0006, 20000808/0007, and 20001005/0016) because they showed spurious ripple patterns. Among the 37 spectra that remained, the highest S/N one was 19960502/0040 (S/N = 484), and the S/N ratios of the others were typically $\sim$100–300. After finding the necessary Doppler shifts (to bring the wavelengths of stellar lines to the laboratory system) in the same manner as mentioned in subsection 2.2 and adjusting the wavelength scale by applying such determined

[11] ⟨http://www.astro.uu.se/~s4n/⟩

[12] ⟨http://atlas.obs-hp.fr/elodie/⟩

Table 4. Sample portion of the predicted line-strength data.

λ (1)	code (2)	species (3)	η_0 [F] (4)	(η_0) [E] (5)	$\chi_{\rm low}$ (6)	$\log gf$ (7)	$\gamma_{\rm rad}$ (8)	$\gamma_{\rm s}$ (9)	$\gamma_{\rm w}$ (10)
3883.080	26.01	Fe2	0.00013	(1.257E−04)	2.029	−7.487	8.54	−6.60	−7.91
3883.081	24.00	Cr1	0.00132	(1.319E−03)	3.887	−0.344	8.33	−5.10	−7.59
3883.205	23.01	V 2	0.00626	(6.263E−03)	1.428	−2.298	8.58	−6.61	−7.86
3883.261	25.00	Mn1	0.00347	(3.468E−03)	5.338	0.644	8.11	−6.10	−7.78
3883.270	24.00	Cr1	0.00104	(1.038E−03)	3.887	−0.448	8.33	−5.08	−7.59
3883.283	26.00	Fe1	0.17365	(1.737E−01)	3.251	−0.600	8.16	−6.06	−7.80
3883.285	28.00	Ni1	0.00001	(1.197E−05)	3.699	−3.536	8.01	−5.43	−7.64
3883.288	24.00	Cr1	0.00595	(5.952E−03)	0.983	−1.210	6.77	−6.39	−7.83
3883.331	24.00	Cr1	0.00071	(7.088E−04)	3.428	−0.854	8.28	−5.15	−7.66
3883.426	23.01	V 2	0.00144	(1.444E−03)	1.673	−2.807	8.36	−6.64	−7.86
3883.440	69.01	Tm2	0.00007	(6.691E−05)	0.029	−0.808	8.17	−6.03	−7.80
3883.478	23.01	V 2	0.00006	(5.907E−05)	6.964	−1.425	8.77	−5.65	−7.66
3883.499	24.01	Cr2	0.00006	(6.079E−05)	11.144	−1.567	8.90	−4.34	−7.39
3883.533	58.01	Ce2	0.00005	(5.169E−05)	0.536	−1.146	8.17	−5.79	−7.72
3883.576	58.01	Ce2	0.00005	(5.134E−05)	0.322	−1.261	8.17	−5.82	−7.73
3883.641	24.00	Cr1	0.00118	(1.181E−03)	3.010	−0.851	7.81	−5.65	−7.81
3883.690	24.00	Cr1	0.00063	(6.313E−04)	3.887	−0.664	8.33	−5.08	−7.59
3883.767	72.01	Hf2	0.00048	(4.773E−04)	1.672	−0.660	8.17	−6.17	−7.84
3883.887	23.00	V 1	0.00002	(2.180E−05)	1.945	−0.787	8.12	−5.66	−7.66
3884.090	22.00	Ti1	0.00011	(1.142E−04)	1.981	−0.986	8.13	−4.38	−7.58

In order to describe the data format of the four files ("idinfo_b.txt", "idinfo_g.txt", "idinfo_r.txt", and "idinfo_i.txt") containing the theoretically predicted line-strengths for help of line-identification at each wavelength region (see subsection 3.2 for more details), the first 20 lines of "idinfo_b.txt" are shown here as an example. The data are presented line by line in the increasing order of wavelength. The meanings of each of the ten columns are as follows: (1) the wavelength in Å, (2) species code following the format used in ATLAS/WIDTH program (e.g., 26.00 for Fe I, 23.01 for V II), (3) species ("Fe1" for Fe I, "V 2" for V II), (4) η_0 (theoretical line(center)-to-continuum opacity ratio evaluated at the depth of $\tau_{5000} \sim 0.2$) expressed in F-format, (5) η_0 expressed in E-format, (6) lower excitation potential (in eV), (7) logarithmic line oscillator strength ($\log gf$), (8) radiation (natural) damping parameter represented by logarithmic radiation damping width ($\log\gamma_{\rm rad}$), (9) Stark effect damping parameter (due to electrons) represented by logarithmic Stark damping width per electron density at 10^4 K ($\log(\gamma_{\rm s}/N_{\rm e})$), and (10) van der Waals damping parameter (due to neutral hydrogen atoms) represented by logarithmic van der Waals damping width per neutral hydrogen density at 10^4 K ($\log(\gamma_{\rm w}/N_{\rm H})$). Note that only those lines with η_0 larger than 10^{-5} are shown here.

corrections,[13] we co-added all 37 spectra to obtain the final spectrum. Finally, continuum-rectification was performed to obtain the normalized spectra for both 19960502/0040 and the co-added one, with which our OAO spectra should be compared.

As can be seen from figures 6a, b, and c (green lines), while the quality of a single ELODIE spectrum (19960502/0040) is insufficient for line-profile studies, even if it is the highest-S/N one available, the superficial S/N ratio can be appreciably improved (up to $\sim$ 1000) by combining all available spectra, which is a promising consequence that extends the potentiality of the ELODIE spectra. It should be kept in mind, however, that co-adding the spectra taken at widely different periods is not desirable in a strict sense, especially when studies of very delicate line-shape differences are involved. As a matter of fact, slight inconsistencies in the line profiles appear to be sometimes observed between our OAO and the co-added ELODIE spectra (e.g., flat-bottom shape vs. bell-like shape, as observed in the Cr II 4616.63 line in figure 6a). Accordingly, care had better be taken in such a high-handedly-improved-S/N spectrum resulting from a combination of all available individual ELODIE spectra.

4.4. BAO Vega Spectrum Atlas

We finally mention the work of Qiu et al. (1999a,b), which is (to our knowledge) the only publication specifically directed to presenting an extensive spectrum atlas of Vega. Their atlas, based on observations at Beijing Astronomical Observatory, is divided into the blue part (4000–6250 Å; Qiu et al. 1999a) and the red part (6250–8450 Å; Qiu et al. 1999b). The resolving power of their spectra is $R \sim 44000$ (blue) and $R \sim 37000$ (red), and the attained signal-to-noise ratio is typically ~ 300, both of which are insufficient for the purpose of studying line profiles (actually the flat-bottom shape of weak lines can not be clearly observed on their spectrum). Yet, this may serve

[13] The applied Doppler corrections (in km s^{-1}) for each of the 37 spectra are as follows: 19940830/0009 (+2.0), 19960502/0040 (+26.6), 19960502/0041 (+26.6), 19960502/0042 (+26.6), 19960502/0043 (+26.6), 19960730/0019 (+8.0), 19961124/0030 (+3.3), 19970916/0008 (0.0), 19970916/0009 (0.0), 19970917/0006 (0.0), 19970918/0014 (0.0), 19970919/0006 (0.0), 19970920/0006 (0.0), 19970921/0006 (0.0), 19970921/0007 (0.0), 19990812/0014 (+5.3), 20000519/0015 (+23.3), 20000519/0016 (+23.3), 20000519/0017 (+23.3), 20000617/0008 (+18.0), 20000617/0009 (+18.0), 20000617/0010 (+18.0), 20001005/0015 (−1.3), 20001007/0012 (0.0), 20001010/0006 (0.0), 20030704/0016 (+13.3), 20030705/0023 (+13.3), 20030706/0019 (+13.3), 20030820/0010 (+3.3), 20030821/0007 (+3.3), 20030917/0011 (0.0), 20030917/0012 (0.0), 20040227/0064 (+24.6), 20040229/0066 (+25.3), 20040326/0062 (+26.6), 20040328/0067 (+26.6), and 20040328/0068 (+26.6).

Table 5. Contents of electronic data files.

subdirectory	filename	size (kB)	section	description
(1)	(2)	(3)	(4)	(5)
fitsfiles	readme.fitsfiles	4	···	explanation for the files in this directory
fitsfiles	obslog_vega.txt	6	2.1	basic data of Vega observations (same as table 1)
fitsfiles	h172167b060502.fits	543	2.2	raw region-b spectrum of Vega
fitsfiles	h172167g060503.fits	341	2.2	raw region-g spectrum of Vega
fitsfiles	h172167r060504.fits	262	2.2	raw region-r spectrum of Vega
fitsfiles	h172167i060501.fits	169	2.2	raw region-i spectrum of Vega
fitsfiles	h172167b060502dn.fits	546	2.2	Dopp.-corr./normalized region-b spectrum of Vega
fitsfiles	h172167g060503dn.fits	341	2.2	Dopp.-corr./normalized region-g spectrum of Vega
fitsfiles	h172167r060504dn.fits	262	2.2	Dopp.-corr./normalized region-r spectrum of Vega
fitsfiles	h172167i060501dn.fits	169	2.2	Dopp.-corr./normalized region-i spectrum of Vega
finalspectra	readme.finalspectra	4	···	explanation for the files in this directory
finalspectra	obspec_b.txt	3108	2.3	finally arranged region-b spectrum of Vega
finalspectra	obspec_g.txt	2384	2.3	finally arranged region-g spectrum of Vega
finalspectra	obspec_r.txt	2137	2.3	finally arranged region-r spectrum of Vega
finalspectra	obspec_i.txt	1689	2.3	finally arranged region-i spectrum of Vega
synthespec	readme.synthespec	3	···	explanation for the files in this directory
synthespec	theocomb_b.txt	3077	3.1	theoretically synthesized region-b spectrum of Vega
synthespec	theocomb_g.txt	2997	3.1	theoretically synthesized region-g spectrum of Vega
synthespec	theocomb_r.txt	3081	3.1	theoretically synthesized region-r spectrum of Vega
synthespec	theocomb_i.txt	3006	3.1	theoretically synthesized region-i spectrum of Vega
lineprediction	readme.lineprediction	4	···	explanation for the files in this directory
lineprediction	idinfo_b.txt	1301	3.2	theoretically predicted line strengths for region b
lineprediction	idinfo_g.txt	789	3.2	theoretically predicted line strengths for region g
lineprediction	idinfo_r.txt	519	3.2	theoretically predicted line strengths for region r
lineprediction	idinfo_i.txt	312	3.2	theoretically predicted line strengths for region i
appendix	readme.appendix	5	···	explanation for the files in this directory
appendix	obslog_regulus.txt	3	appendix 1	basic data of Regulus observations
appendix	h087901b060502.fits	543	appendix 1	raw region-b spectrum of Regulus
appendix	h087901g060503.fits	341	appendix 1	raw region-g spectrum of Regulus
appendix	h087901r060504.fits	262	appendix 1	raw region-r spectrum of Regulus
appendix	h087901i060501.fits	169	appendix 1	raw region-i spectrum of Regulus
appendix	h087901b060502Dn.fits	546	appendix 1	Dopp.-corr./normalized region-b spectrum of Regulus
appendix	h087901g060503Dn.fits	341	appendix 1	Dopp.-corr./normalized region-g spectrum of Regulus
appendix	h087901r060504Dn.fits	262	appendix 1	Dopp.-corr./normalized region-r spectrum of Regulus
appendix	h087901i060501Dn.fits	169	appendix 1	Dopp.-corr./normalized region-i spectrum of Regulus

Information of the electronic data files is summarized here, which are downloadable from the URL described in the footnote to the title on the top page: (1) name of the subdirectory, (2) file name (all files except for those named as "*.fits" are ascii/text files), (3) file size (in kB), (4) section number in the main text where the relevant explanation is presented, and (5) the brief description of the file contents.

as a useful data source for conventional abundance analyses based on equivalent widths. Unfortunately, their spectra are published only in the classical form of printed figures in a journal paper without providing any access to actual digital data, by which the usability of this atlas is rather limited.

5. Summary

Considering that no very-high S/N ($\gtrsim$1000–2000) spectrum of Vega is available in the public domain, in spite of the necessity of such a high-quality database for studying the unusual profiles of weak lines to verify/clarify the "pole-on-seen rapid rotator" picture of this star, we published in this study a high-dispersion and high-S/N spectrum atlas of Vega based on the observations at Okayama Astrophysical Observatory. Our spectra, covering the wavelength region of 3900–8800 Å (though with a gap at 7200–7600 Å), have such a high resolution ($R \sim 100000$) and high signal-to-noise ratio (typically $\sim$ 1000–2000 on the average) as to allow a detailed line-profile analysis.

In addition, in order to help increase the usability of the atlas, we also presented theoretically simulated spectra as well as a list of lines predicted to have appreciable strengths, both obtained as the result of spectrum synthesis calculations, so that they may be of help in identifying lines, or finding suitable lines on the actual spectra.

All of these observational and theoretical data are available in the form of electronic data, which can be downloaded via the Internet (see the URL described in the footnote to the title on the top page). A summary of these on-line data is given in table 5 for the readers' convenience.

The spectra obtained in this study were compared with those

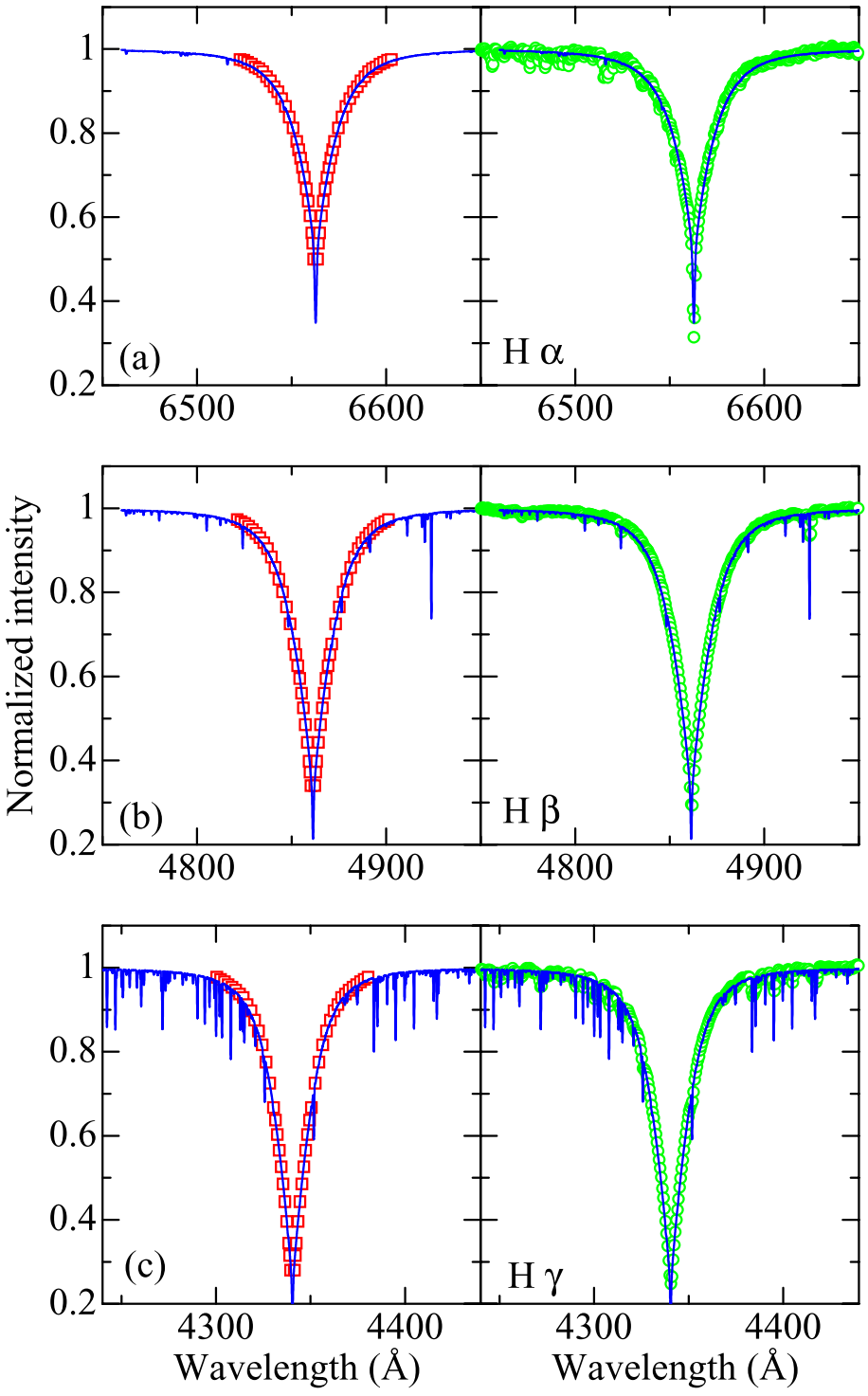

Fig. 8. Comparison of our computed theoretical profiles (H_λ^{20}/H_c given in the "theocomb_?.txt" files, corresponding to $T_{\rm eff} = 9550$ K, $\log g = 3.95$, and [X/H] = −0.5, $v_t = 2\,{\rm km\ s^{-1}}$, and $v_e \sin i = 20\,{\rm km\ s^{-1}}$) and the (published) observed profiles for three representative Balmer lines; (a) H α, (b) H β, and (c) H γ. While the theoretical profiles are depicted in (blue) solid lines, the observational data are shown by symbols: (red) open squares in the left panels are the Balmer line contours published Peterson (1969) and (green) open circles in the right panels are the low-resolution CCD spectra published by Sadakane et al. (2003). [Colored only in the electronic edition.]

of several other groups published so far. In a comparison with the ultra-high S/N spectrum reported by Gulliver et al. (1991) in their pioneering work, which we targeted in conducting this project, our S/N ratio ($\sim$ 1500–2000) somewhat falls behind their achievement ($\gtrsim$ 2500), as far as the wavelength region they used (around $\sim$ 4500 Å) is concerned. In any case, we consider that our spectra, covering a wider wavelength region than theirs, equally have a sufficiently high quality, such as to be applicable to studying detailed features of weak-line profiles (e.g., "flat-bottom" shape).

Regarding the other public-domain Vega spectra available on-line, those of the S^{4}N project (Allende Prieto et al. 2004) and the ELODIE spectrum library (Moultaka et al. 2004), they do not appear to be suitable for investigating the detailed profile of spectral lines because of the lack of sufficiently-high S/N ratios (though the S/N in the ELODIE case may be improved by co-adding all available spectra), while they still serve as quite a useful database for simple line-strength measurements. The same argument also holds for Qiu et al.'s (1999a,b) Beijing Astronomical Observatory spectrum atlas of Vega (available only in the hardcopy form).

By using these spectra published here, we are currently undertaking detailed line-shape analyses (with the help of spectrum simulations based on the gravity-darkened Roche model) toward the purpose of establishing the stellar rotation parameters ($v_{\rm e}$ and i) of Vega, such as was done by Gulliver et al. (1994) or Hill et al. (2004). The results will be published in the near future.

The authors are indebted to Dr. H. Izumiura for helpful suggestions toward an achievement of very-high S/N observations.

Appendix 1. Spectra of Regulus as a Reference of Telluric Lines

In using the digital spectrum atlas of Vega published in this study, nuisance features are the numerous telluric lines caused by absorptions in the Earth's atmosphere (mainly due to H_2O and O_2 molecules). Actually, as can be seen in figures 1 and 2, the contamination of such lines becomes progressively significant toward longer wavelength regions. The easiest way to identify these lines is to look at the spectrum of a rapidly rotating star with large $v_{\rm e}\sin i$, since there should be no confusion with stellar lines, which are mostly smeared out because of the considerable Doppler broadening caused by rapid rotation.

Accordingly, for such a reference purpose of telluric lines, we also append the spectra of Regulus (= α Leo = HR 3982 = HD 87901 = HIP 49669, B7 V), which is a representative rapid rotator with a large $v_{\rm e}\sin i$ value of 300 km s^{-1} (Abt et al. 2002), since we also observed this star just before Vega on each night of May 1–4, and the spectra for each of the four regions (b, g, r, and i) are at our hand (cf. footnote 1).

Analogous to the case of Vega, eight fits-formatted files (raw and reduced[14] spectra of Regulus for each of the four wavelength regions) are available in the "appendix" directory of the electronic data table (cf. table 5), where the file "obslog_regulus.txt" (describing the observation logs and information of each individual spectrum frame of Regulus) is also presented.

One possible application of these Regulus spectra may be to remove the telluric feature in the Vega spectra by using a special tool, such as the "telluric" task in IRAF. For this purpose, information on the appropriate value of air-mass for the relevant spectrum is necessary, on which the strengths of telluric lines depend. The weighted-mean air-mass values for the two stars observed at the same night ($\langle \sec z \rangle_{\rm vega}$, $\langle \sec z \rangle_{\rm regulus}$) are (1.03, 1.15), (1.33, 1.24), (1.28, 1.15), and (1.29, 1.21) on May 1 (region i), 2 (region b), 3 (region g), and 4 (region r), respectively. Figure 7 shows an example of such a devision applied to the aperture No.1 segment (7040–7165 Å) of the region-r spectra (May 4) for Vega (h172167r060504dn.fits) and Regulus (h087901r060504Dn.fits) with the "telluric" task.[15] We can see from this figure that this removal process turned out to be successful with a clean recovery of the C I lines at 7110–7120 Å. It should be kept in mind, however, that such a successful division can not be generally expected when the telluric lines are numerous and very strong.

Appendix 2. Reliability of the Computed Hydrogen Line Profiles

As mentioned in subsection 2.3, the last step of arranging the final spectra ("obspec_?.txt" files) was done by comparing the combined tentatively normalized spectra ("h172167?06050?dn.fits" files) with the simulated theoretical spectra ("thecomb_?.txt" files), since it was hardly possible in our case of segmented echelle spectra to perform a reliable continuum-normalization in the region of hydrogen lines showing very broad (or mutually overlapping) wings. In order to assure the reliability of this procedure, however, it has to be confirmed in advance that our computations of hydrogen lines with the ($T_{\rm eff}$ = 9550 K, $\log g$ = 3.95, [M/H] = -0.5) model atmosphere reliably reproduce the observational profiles of Vega.

For this purpose, we decided to compare our calculations with reference observational profiles (H α, H β, and H γ) taken from two different sources: (i) the reduced profiles published by Peterson (1969) and (ii) Sadakane et al.'s (2003[16]) low-resolution normalized spectra, which were observed with a normal grating over a wide wavelength range, and thus a reliable location of the continuum level is feasible.[17] The results are shown in figure 8, where we can see that our theoretical Balmer line profiles satisfactorily match the observed data, except for some slight inconsistencies in the far wing (e.g., the case for H γ), which can be ascribed to a person-to-person difference in the manner of continuum placement. Thus, we may state that our final normalization adjustment by invoking the theoretically computed spectra is reasonably valid.

[14] Note that the Doppler correction in this case was chosen to be the same as that adopted in the corresponding Vega spectrum (cf. subsection 2.2), because we intended to make the positions of *telluric lines* in the resulting Regulus reduced spectrum (e.g., h087901r060504Dn.fits) coincide with those in the corresponding Vega reduced spectrum (h172167r060504dn.fits). (This is markedly different from the case for Vega, where the applied Doppler correction was to bring the stellar lines to the laboratory positions.) This is the reason why we used the character 'D' (instead of 'd') to emphasize this difference.

[15] Practically, this can be executed by typing "telluric h172167r060504dn.fits[*,1] *output.fits* h087901r060504Dn.fits[*,1]", while giving the air-mass value of 1.29 and 1.21 in response to the prompt. Then, the resulting spectrum is written in the file "*output.fits*."

[16] ⟨http://galaxy.cc.osaka-kyoiku.ac.jp/atlas/STORY/kenkyuu/starlist/list19.html⟩

[17] Sadakane et al.'s (2003) Vega spectra consist of the red spectrum (for H α) and the blue spectrum (for H β and H γ), each has a wavelength-resolution/coverage of $R \sim 6000/\sim 600$ Å and $R \sim 3000/\sim 1000$ Å, respectively.

References

Abt, H. A., Levato, H., & Grosso, M. 2002, ApJ, 573, 359

Abt, H. A., & Morrell, N. I. 1995, ApJS, 99, 135

Allende Prieto, C., Barklem, P. S., Lambert, D. L., & Cunha, K. 2004, A&A, 420, 183

Castelli, F., & Kurucz, R. L. 1994, A&A, 281, 817

Elste, G. H. 1992, ApJ, 384, 284

Griem, H. R. 1960, ApJ, 132, 883

Griem, H. R. 1967, ApJ, 147, 1092

Gulliver, A. F., Adelman, S. J., Cowley, C. R., & Fletcher, J. M. 1991, ApJ, 380, 223

Gulliver, A. F., Hill, G., & Adelman, S. J. 1994, ApJ, 429, L81

Hill, G., Gulliver, A. F., & Adelman, S. J. 2004, in IAU Symp. 224, The A-Star Puzzle, ed. J. Zverko, J. Žižňovský, S. J. Adelman, & W. W. Weiss (Cambridge: Cambridge University Press), 35

Izumiura, H. 1999, in Proc. 4th East Asian Meeting on Astronomy, Observational Astrophysics in Asia and its Future, ed. P. S. Chen (Kunming: Yunnan Observatory), 77

Kato, K.-I., Ono, N., Terasaki, S., Masui, K., & Sadakane, K. 2000, Publ. Osaka Sci. Mus., 10, 7

Kurucz, R. L. 1970, Smithsonian Astrophysical Observatory Special Report, No.309

Kurucz, R. L. 1993, Kurucz CD-ROM, No. 13 (Harvard-Smithsonian Center for Astrophysics)

Kurucz, R. L., & Bell, B. 1995, Kurucz CD-ROM, No. 23 (Harvard-Smithsonian Center for Astrophysics)

Lemke, M. 1997, A&AS, 122, 285

Leushin, V. V., & Topil'skaya, G. P. 1987, Astrophysics, 25, 415

Moultaka, J., Ilovaisky, S. A., Prugniel, Ph., & Soubiran, C. 2004, PASP, 116, 693

Pagel, B. E. J. 1997, Nucleosynthesis and Chemical Evolution of Galaxies (Cambridge: Cambridge University Press), ch.3

Peterson, D. M. 1969, Smithsonian Astrophysical Observatory Special Report, No.293

Peterson, D. M., et al. 2006, Nature, 440, 896

Qiu, H., Zhao, G., Chen, Y., & Li, Z. 1999a, Publ. Beijing Astron. Obs., 33, 34

Qiu, H., Zhao, G., & Li, Z. 1999b, Publ. Beijing Astron. Obs., 33, 58

Royer, F., Grenier, S., Baylac, M.-O., Gómez, A. E., & Zorec, J. 2002, A&A, 393, 897

Sadakane, K., et al. 2003, Astron. Her., 96, 392 (in Japanese)

Takeda, Y. 1993, in Peculiar versus Normal Phenomena in A-type and Related Stars, Proc. IAU Colloq. 138, ed. M. M. Dworetsky, F. Castelli, & R. Faraggiana (San Francisco: Astronomical Society of the Pacific), 491

Takeda, Y., et al. 2002, PASJ, 54, 113

Takeda, Y., et al. 2005, PASJ, 57, 13

Vidal, C., Cooper, J., & Smith, E. W. 1973, ApJS, 25, 37